Theoretical Study of Solvent Effects on the Thermodynamics of Iron(III) [Tetrakis(pentafluorophenyl)]porphyrin Chloride Dissociation

Rustam Z. Khaliullin,[†,‡] Martin Head-Gordon,[†,‡] and Alexis T. Bell*[,†,§]

Chemical Sciences Division, Lawrence Berkeley National Laboratory, Berkeley, California 94720, Department of Chemistry and Department of Chemical Engineering, University of California, Berkeley, California 94720

Received: May 9, 2007; In Final Form: July 11, 2007

A quasichemical method that combines ab initio treatment of explicit solvent with dielectric continuum models has been used to study the origin of a strong effect of methanol on the extent of iron(III) [tetrakis-(pentafluorophenyl)]porphyrin chloride dissociation in acetonitrile−methanol solutions. It is shown that the dissociation is energetically more favorable in methanol than in acetonitrile primarily because of the strong specific interactions between the chloride anion and the solvent methanol molecules in its first solvation shell. These interactions are weaker in acetonitrile. The final estimate for the difference in the dissociation free energies in methanol and acetonitrile is −23 kJ/mol, in a good agreement with the experimental value of −21 kJ/mol. Energy decomposition analysis of chloride−solvent interactions suggests that stronger chloride−methanol binding is a result of the contribution of charge delocalization effects to the chloride−methanol interactions.

1. Introduction

It has been shown recently that iron(III) [tetrakis(pentafluorophenyl)]porphyrin chloride, here abbreviated as PFeCl (Figure 1), is catalytically inactive for cyclooctene epoxidation by hydrogen peroxide or hydrogen peroxide decomposition when dissolved in acetonitrile but is active if the solvent contains methanol.[1,2] Evidence based on shifts in the position of the ^{1}H NMR signal of the β-pyrrole protons on the porphyrin ring suggests that the role of methanol is to facilitate the dissociation of PFeCl into PFe^+ and Cl^-. It was also found that the dissociation process involves axial coordination of methanol to the iron(III) center located at the center of the porphyrin ring, to form $PFe(MeOH)^+$. The kinetics of cyclooctene epoxidation by hydrogen peroxide was found to be linear in the concentration of $PFe(MeOH)^+$, where the concentration of this cation was determined from the equilibrium constant for the following reaction:

$$PFeCl_{sol} + MeOH_{sol} \rightleftharpoons PFe(HOMe)_{sol}^{+} + Cl_{sol}^{-} \qquad (R1)$$

The equilibrium constant for this reaction in the mixture of methanol and acetonitrile, K_{mix}, was described by the following equation:

$$K_{mix} = \exp\left(-\frac{(\Delta H^\circ_{MeCN} + \alpha[MeOH])}{RT} + \frac{\Delta S^\circ}{R}\right) \qquad (1)$$

where ΔH°_{MeCN} is the enthalpy of PFeCl dissociation in pure acetonitrile, α is a factor indicating the extent to which the enthalpy of dissociation changes with increasing molar concentration to methanol, [MeOH] is the molar concentration of methanol, and ΔS° is the entropy of PFeCl dissociation.

Values of ΔH°_{MeCN}, α, and ΔS° were determined by fitting eq 1 to values of K_{mix} obtained from ^{1}H NMR measurements made for various solvent compositions and temperatures. The resulting values were $\Delta H^\circ_{MeCN} = 25.1 \pm 1.3$ kJ/mol, $\Delta S^\circ = -24.7 \pm 3.3$ J/K·mol, and $\alpha = -0.84 \pm 0.04$ kJ·L/mol^2. Using these values, it was established that the change in Gibbs free energy for reaction R1 is 20.7 ± 1.0 kJ/mol lower in pure methanol than in pure acetonitrile; that is,

$$\Delta\Delta G^\circ \equiv \Delta G^\circ_{MeOH} - \Delta G^\circ_{MeCN} = -20.7 \pm 1.0 \text{ kJ/mol} \qquad (2)$$

The strong effect of methanol on the extent of PFeCl dissociation in acetonitrile−methanol solutions was attributed to the ability of methanol to stabilize the products of dissociation.[2] However, it was not possible solely on the basis of experimental evidence to determine the extent to which methanol enhances the dissociation of the porphyrin salt as a consequence of coordination to PFe^+ versus its effects on the solvation of $PFe(MeOH)^+$ and Cl^-. The aim of this paper is to isolate these effects through the use of ab initio methods. In carrying out this study, we have found that a quasichemical model provides a relatively simple and the most effective means for determining the effects of solvent composition on $\Delta\Delta G^\circ$.

2. Models and Methods

The standard free energy change of reaction R1 in solvent S is a sum of two components: the ideal gas free energy change and the excess free energy change.

$$\Delta G^\circ_S = \Delta G^\circ_{ig} + \Delta G^\circ_{ex,S} \qquad (3)$$

ΔG°_{ig} is the free energy change for reaction R1 occurring in the gas phase and in the absence of solvation effects, whereas $\Delta G^\circ_{ex,S}$ is the free energy change due to differences in the solvation of reactants and products:

* Corresponding author. E-mail: alexbell@berkeley.edu.
† Lawrence Berkeley National Laboratory.
‡ Department of Chemistry.
§ Department of Chemical Engineering.

10.1021/jp073557a CCC: $37.00
Published on Web 08/28/2007

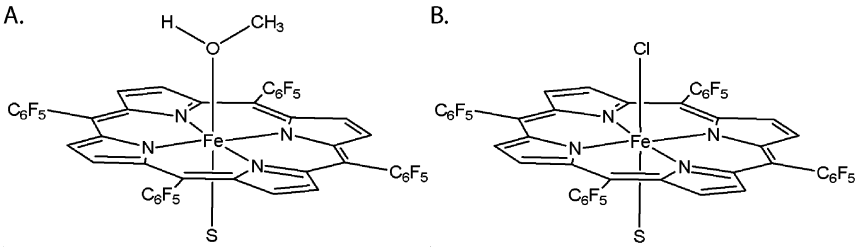

Figure 1. Iron(III) [tetrakis-(pentafluorophenyl)]porphyrin systems with two axial ligands: (A) S·PFe(HOMe)$^+$ and (B) S·PFeCl. S = MeOH and MeCN. The methanol molecule is coordinated through the oxygen atom; the acetonitrile molecule is coordinated through the nitrogen atom.

$$\Delta G^\circ_{ex,S} = \Delta G^\circ_{ex,S}(Cl^-) + \Delta G^\circ_{ex,S}(PFe(HOMe)^+) - \Delta G^\circ_{ex,S}(PFeCl) - \Delta G^\circ_{ex,S}(MeOH) \quad (4)$$

$\Delta G^\circ_{ig}(X)$ is the ideal gas free energy of species X, and $\Delta G^\circ_{ex,S}(X)$ is the excess free energy of species X in solvent S.

Using eqs 3 and 4, the difference $\Delta\Delta G^\circ$ defined in eq 2 can be written as a sum of four terms (the ideal gas term is the same for both solvents):

$$\Delta\Delta G^\circ = \Delta\Delta G^\circ_{ex}(Cl^-) + \Delta\Delta G^\circ_{ex}(PFe(HOMe)^+) - \Delta\Delta G^\circ_{ex}(MeOH) - \Delta\Delta G^\circ_{ex}(PFeCl) \quad (5)$$

Comparison of the solvation energies of the species involved in reaction R1 in methanol and acetonitrile will elucidate the principal effects and the role of solvent composition on the energetics of PFeCl dissociation.

Calculation of accurate solvation free energies for ions and molecules, right hand side of eq 4, is a fundamental problem in theoretical chemistry. The most accurate approaches to this problem are molecular dynamics or Monte Carlo simulations with explicit solvent that sample the most important configurations of solvent molecules around the solute.[3] In combination with free energy perturbation or thermodynamic integration techniques,[3−5] these methods are capable of producing reasonable solvation free energies provided that sufficiently long trajectories are generated, a large enough solvent box with periodic boundaries is used, and the potential energy surface is adequately described (i.e., all pertinent inter- and intramolecular interactions are accounted).[6,7]

Empirical force fields are the cheapest but not always the most accurate method to evaluate the total energy along the sampled trajectory.[8,9] Ab initio electronic structure theory gives an accurate description of solvent−solute and solvent−solvent interactions but becomes very expensive for systems of many solvent molecules and long trajectories. For charged species (i.e., the chloride anion and porphyrin cation in this work), there is also a principal issue of the treatment of long-range electrostatic interactions in the context of a sample of finite size.[10,11] These factors place severe limitations on the use of ab initio simulations with explicit treatment of solvent molecules for free energy calculations.

Continuum-based or implicit-solvent models that incorporate solvent effects into quantum mechanical calculations of the solute represent a practical alternative to explicit-solvent models.[12−14] In this conceptually simple framework, the solute molecules are embedded in a cavity in the continuum characterized by its dielectric constant. The charge distribution (electrons and nuclei) of the solute, inside the cavity, polarizes the dielectric continuum, which in turn polarizes the solute charge distribution. A number of techniques has been developed to find the energy of the final self-consistent polarized charge distributions.[14] Long-range effects which are of a great importance for charged solutes are properly taken into account in the polarizable continuum models.[10] Ambiguities arise in the definition of the solute cavity and treatment of nonelectrostatic effects such as cavitation, dispersion, and specific solute−solvent interactions.

Since methanol and acetonitrile have similar dielectric constants ($\epsilon_{MeOH} = 32.6$, $\epsilon_{MeCN} = 36.6$),[15] the strong solvent effect on the dissociation of PFeCl is unlikely to be explained by a continuum model. The possibility of combining explicit solvation techniques with the dielectric continuum representation in the same calculation has been the topic of a number of recent studies.[14,16−22] The main idea of these discrete/continuum (or explicit/implicit) models is to include a small number of solvent molecules explicitly, usually those belonging to the first solvation shell, and then describe the remaining solvent as a dielectric continuum. One of the advantages of mixed discrete/continuum models is that they do not require lengthy sampling of the solvent configuration phase space because the number of degrees of freedom that need to be treated explicitly is greatly decreased.

The statistical mechanical foundation of the mixed discrete/continuum models has been summarized by Paulaitis and Pratt.[23] These models are most commonly referred to as quasichemical models. Ideally, the best description of the first explicit shell includes averaging over all possible configurations of solute and solvent, with all possible numbers of solvent molecules in the cluster. However, for practical reasons, the most primitive form of the quasichemical theory takes into account only the most stable configuration of the cluster.[17,20]

In the simplest form of the quasichemical approximation,[17,20] the solvation free energy (the excess chemical potential) of solute X is expressed in terms of the solvation free energy of the cluster, $\Delta G^\circ_{ex,S}(S_n{\cdot}X)$ and the gas-phase free energy of the cluster formation, $\Delta G^\circ_{ig,form}(S_n{\cdot}X)$:

$$\Delta G^\circ_{ex,S}(X) = \Delta G^\circ_{ig,form}(S_n{\cdot}X) + \Delta G^\circ_{ex,S}(S_n{\cdot}X) - n\Delta G^\circ_{ex,S}(S) - nRT\ln[S] \quad (6)$$

where $\Delta G^\circ_{ig,form}(S_n{\cdot}X)$ is given by:

$$\Delta G^\circ_{ig,form}(S_n{\cdot}X) = \Delta G^\circ_{ig}(S_n{\cdot}X) - \Delta G^\circ_{ig}(X) - n\Delta G^\circ_{ig}(S) \quad (7)$$

The energetics of specific solute−solvent interactions are described by $\Delta G^\circ_{ig,form}(S_n{\cdot}X)$, whereas $\Delta G^\circ_{ex,S}(S_n{\cdot}X)$ includes long-range interactions and is calculated with a dielectric continuum model. The first three terms of eq 6 can be interpreted as the free energies of three elementary steps in which a gas phase solute particle (molecule or ion) is placed into the solvent. In the first step, *n* solvent molecules S are removed from the solvent to the gas phase (term 3), then *n* solvent molecules interact with the solute in the gas phase to form cluster $S_n{\cdot}X$ (term 1), and finally the cluster is placed into the solvent (term

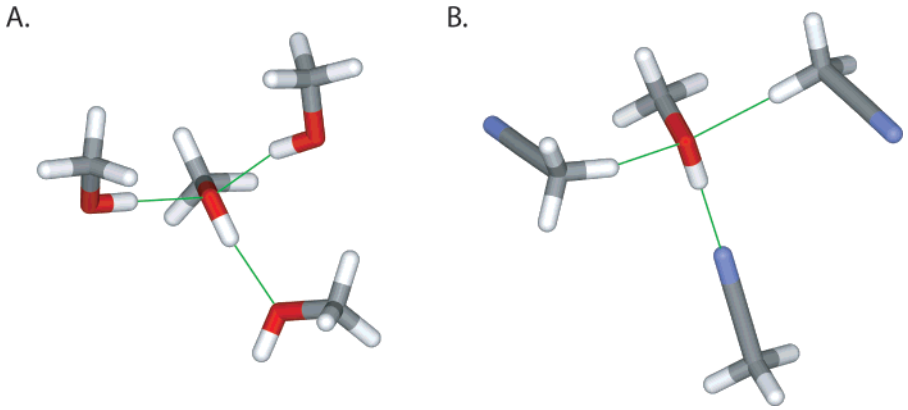

Figure 2. Methanol molecule in (A) methanol and (B) acetonitrile.

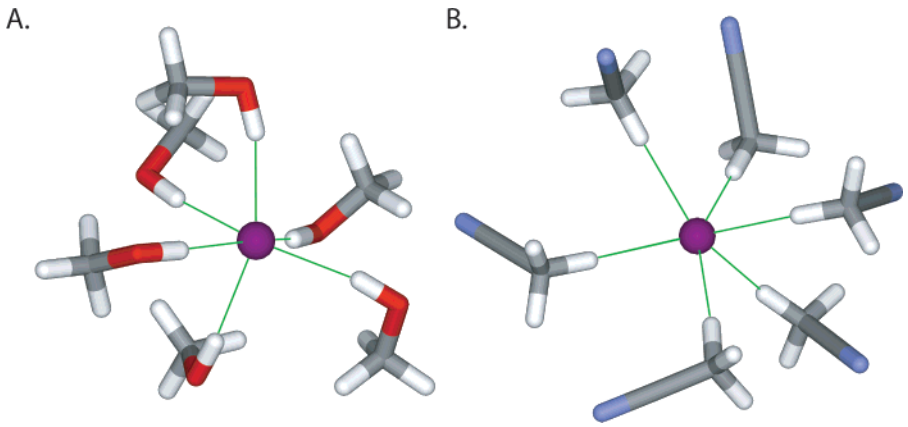

Figure 3. Chloride anion interacting with six solvent molecules: (A) methanol and (B) acetonitrile.

2). The fourth term in eq 6 is a correction for the solvent concentration.[17,18,20,23]

Equation 6 is used in this work to estimate the difference in the free energies of solvation of the species involved in reaction R1 and, finally, the difference in the standard free energy change of reaction R1 in methanol and acetonitrile, $\Delta\Delta G^\circ$.

The first solvation shell of the porphyrin system contains too many solvent molecules (of the order of several tens) to be readily tractable with modern ab initio methods, particularly since this large shell is likely to exhibit significant variability. Therefore, only one solvent molecule for which specific nonelectrostatic interactions with the porphyrin might be different in the two different solvents was included explicitly in the quantum chemical region. This solvent molecule interacts directly with the Fe ion as its second axial ligand (Figure 1). To account for specific solvation of the methanol molecule on the left side of reaction R1, clusters with three explicit solvent molecules are used. Two solvent molecules form hydrogen bonds with the lone pairs of the methanol oxygen atom; the third solvent molecule interacts with the hydrogen atom of the methanol hydroxyl (Figure 2). We think that this solvent configuration is the most stable one and that the remaining solute−solvent interactions can be captured with the dielectric continuum. We have used different numbers of solvent molecules to describe short-range interaction of the solvent with the chloride anion. Figure 3 shows clusters with six explicit solvent molecules.

Calculation of the ideal gas free energy of the cluster formation, $\Delta G^\circ_{ig,form}(S_n{\cdot}X)$ in eq 6, is complicated by the presence of many degrees of freedom that correspond to low-frequency vibrations and hindered rotations of solute and solvent molecules relative to each other. The standard treatment of these highly anharmonic floppy modes as harmonic vibrations results in large errors in $\Delta G^\circ_{ig}(S_n{\cdot}X)$. To avoid this problem, we used a rigid-molecule model. The error introduced into the absolute values of the solvation free energies by the use of this approximation grows with the number of solvent molecules in the cluster, n, as more and more low-frequency modes are neglected. Inclusion of the thermal correction for rotations and translations has a great impact on the absolute values of the solvation free energies; however, the $\Delta\Delta G^\circ_{ex}(X)$ is almost unaffected by translations and rotations. To illustrate this, we used two models to approximate $\Delta G^\circ_{ig,form}(S_n{\cdot}X)$. In model 1, $\Delta G^\circ_{ig,form}(S_n{\cdot}X)$ is approximated by the total electronic energy change. Thus, all ideal gas-phase entropy contributions (rotations, translations, and vibrations) are completely neglected. In model 2, the electronic energy change is combined with the thermal correction for rotational and translational degrees of freedom.

The Q-CHEM 3.0 software package[24] was used to perform geometry optimization and to evaluate all final electronic energies. Calculations for the porphyrin systems were done using the EDF1 density functional[25] and the 6-31G basis set. Calculations for the chloride anion and methanol are done at the MP2/6-31(+,+)G(d, p) level.[26,27] The basis-set superposition error (BSSE) was removed from all intermolecular interaction energies by the counterpoise method.[28] Thermodynamic functions for all species were evaluated using standard ideal gas statistical mechanics equations.[29] $T = 298.15$ K was used throughout. Note that (°) refers to the 1 M standard state.[30] Most

TABLE 1: Gas-Phase Calculations for Porphyrins

	doublet	quartet	sextet
	$\langle S^2\rangle$[a]		
PFeCl	1.0962	3.7822	8.7563
MeOH·PFeCl	0.7962	3.7853	8.7567
MeCN·PFeCl	0.7796	3.7833	8.7562
$PFe(HOMe)^+$	1.1042	3.7823	8.7552
$MeOH·PFe(HOMe)^+$	0.7850	3.7881	8.7548
$MeCN·PFe(HOMe)^+$	0.7710	3.7877	8.7558
	Energy relative to quartet, kJ/mol		
PFeCl	48.1	0.0	10.2
MeOH·PFeCl	18.3	0.0	23.6
MeCN·PFeCl	6.7	0.0	11.9
$PFe(HOMe)^+$	79.1	0.0	41.8
$MeOH·PFe(HOMe)^+$	39.4	0.0	42.1
$MeCN·PFe(HOMe)^+$	16.2	0.0	39.9

[a] Exact values of $\langle S^2\rangle$ should be 0.75, 3.75, and 8.75 for doublet, quartet, and sextet, respectively. Calculated values are expectation values of the Kohn−Sham wavefunction which are of diagnostic use but are not true $\langle S^2\rangle$ values.

quantum chemistry software packages calculate ideal gas thermodynamic functions for the 1 atm standard state (•). The transformation between the states is:

$$\Delta G^\circ_{ig}(X) = \Delta G^\bullet_{ig}(X) + RT\ln[\tilde{R}T] \quad (8)$$

where $\tilde{R} = 0.082\,058\ K^{-1}$.

Nonspecific solvation energies are calculated with the surface and simulation of volume polarization for electrostatics polarizable continuum model, or SS(V)PE for short, developed by Chipman.[31] The SS(V)PE model treats the solvent as a continuum dielectric, solving Poisson's equation for apparent surface charges on the solute cavity surface which is defined as the isodensity countour of 0.0025 au. SS(V)PE was designed to provide a good approximation to the volume polarization arising from "escaped charge", which is the fraction of the wavefunction extending past the cavity boundary. SS(V)PE calculations were performed at the EDF1/6-31G level for PFeCl and $PFe(HOMe)^+$ and at the HF/6-31(+,+)G(d, p) level for chloride and methanol. Dielectric constants are $\epsilon_{MeOH} = 32.6$ and $\epsilon_{MeCN} = 36.6$.[15]

We further examine the detailed origin of the interaction of chloride with solvent molecules by decomposing the intermolecular binding energy into physically relevant components such as the contribution from interacting "frozen monomer densities" (FRZ), the energy lowering due to polarization (POL) of the densities (without charge transfer), and the further energy lowering due to charge transfer (CT) effects. This is accomplished using a recently introduced energy decomposition analysis (EDA) scheme based on absolutely localized molecular orbitals.[32] Since the application of the energy decomposition method is limited to single determinant wavefunctions computed with DFT methods, we applied EDA to the interaction energies calculated with a series of density functionals which most closely reproduce more accurate MP2 energies. The EDA results are reported for B3LYP,[33,44] BLYP,[34,35] BP86,[35,36] BMK,[37] PW91,[38] and EDF2[39] density functionals. All EDA calculations use 6-31(+,+)G(d, p) basis set and MP2/6-31(+,+)G(d, p) geometries.

3. Results and Discussion

3.1. $\Delta\Delta G^\circ_{ex}$(PFeCl) and $\Delta\Delta G^\circ_{ex}$($PFe(HOMe)^+$). All gas-phase calculations for PFeCl and $PFe(HOMe)^+$ were performed for doublet, quartet, and sextet spin states. $\langle S^2\rangle$ values (Table 1) indicate that spin contamination is not significant for the quartet and the sextet states. Doublet wavefunctions are more spin contaminated. However, since the quartet states are the most stable for all porphyrin species considered in this work (Table 1), we did not attempt spin state purification for doublets as the purification only increases the total energy. We used results for the quartet states in all further calculations.

The energies of solvation of porphyrin systems calculated according to eq 6 are shown in Table 2. The ideal gas-phase energy of cluster formation are calculated with and without the thermal corrections for rotations and translations (model 2 and model 1). However, $\Delta\Delta G^\circ_{ex}$ is the same for both models. Both the neutral porphyrin chloride and the porphyrin cation are better stabilized in methanol than in acetonitrile: $\Delta\Delta G^\circ_{ex}(PFeCl) = -6$ kJ/mol, and $\Delta\Delta G^\circ_{ex}(PFe(HOMe)^+) = -9$ kJ/mol. This is mostly because the methanol as an axial ligand better stabilizes the porphyrin system than does acetonitrile: $\Delta\Delta G^\circ_{ig,form}$ is around −12 kJ/mol. As expected, the long-range electrostatic effect is the same for methanol and acetonitrile: $\Delta\Delta G^\circ_{ex,S}$ for porphyrin systems is zero. The cation is better stabilized by the polarizable continuum than the neutral PFeCl system is.

3.2. $\Delta\Delta G^\circ_{ex}(Cl^-)$. $\Delta G^\circ_{ex,S}(Cl^-)$ is calculated for both methanol and acetonitrile according to eq 6. Results of the calculations for different numbers of explicit solvent molecules, $n = 0-6$, are shown in Table 3. Again, absolute values of $\Delta G^\circ_{ig,form}(S_n{\cdot}Cl^-)$ calculated with model 1 and model 2 are significantly different (see comment on the absolute free energy values below); however, the ΔΔ quantities for models 1 and 2 ($\Delta\Delta G^\circ_{ex}(Cl^-)$, $\Delta\Delta G^\circ_{ig,form}(S_n{\cdot}Cl^-)$, $\Delta\Delta S^\circ_{ig,form}(S_n{\cdot}Cl^-)$) are almost the same.

To obtain $\Delta\Delta G^\circ_{ex}(Cl^-)$, we compared results for methanol and acetonitrile with the same number of explicit solvent molecules. As was mentioned before, the error in the calculated absolute values of the solvation energies depends on the number of explicit solvent molecules in the cluster. Therefore, the most accurate values of $\Delta\Delta G^\circ_{ex}(Cl^-)$ are obtained by subtracting the absolute values of $\Delta G^\circ_{ex,S}(Cl^-)$ computed for the same value of *n*.

The polarizable continuum model alone ($n = 0$) predicts virtually no difference in the energetics of chloride solvation in two solvents because of the very similar dielectric constants

TABLE 2: Energetics (kJ/mol) of Porphyrin Solvation in Methanol and Acetonitrile (X = PFeCl and X = $PFe(HOMe)^+$) with Gas Phase, and SS(V)PE Calculations Are Performed at EDF1/6-31G Level of Theory; Quartet Spin States Are Used

	$\Delta G^\circ_{ig,form}$ (S·X) model 1[a]	$\Delta G^\circ_{ig,form}$ (S·X) model 2[b]	$\Delta G^\circ_{ex,S}$ (S·X)	$-\Delta G^\circ_{ex,S}(S)$	$-RT\ln[S]$	$\Delta\Delta G^\circ_{ex,S}$ (X) model 1[a]	$\Delta G^\circ_{ex,S}$ (X) model 2[b]
MeOH·PFeCl	−22	27	−118	26	−8	−122	−72
MeCN·PFeCl	−11	39	−118	21	−7	−115	−66
Δ (MeOH−MeCN)	−11	−12	1	5	−1	−6	−6
$MeOH·PFe(HOMe)^+$	−60	−9	−294	26	−8	−336	−285
$MeCN·PFe(HOMe)^+$	−47	4	−294	21	−7	−327	−276
Δ (MeOH−MeCN)	−13	−13	0	5	−1	−9	−9

[a] Model 1 includes only electronic degrees of freedom. [b] Model 2 includes electronic, rotational, and translational degrees of freedom.

TABLE 3: Energetics (kJ/mol) of Chloride Solvation in Methanol and Acetonitrile (X = Cl^-) with Gas Phase, and SS(V)PE Calculations Are Performed at MP2/6-31(+,+)G(d, p) and HF/6-31(+,+)G(d, p) Levels of Theory, Respectively

	$\Delta G^\circ_{ig,form}(S_n\cdot X)$ model 1[a]	$\Delta G^\circ_{ig,form}(S_n\cdot X)$ model 2[b]	$\Delta G^\circ_{ex,S}(S_n\cdot X)$	$-n\Delta G^\circ_{ex,S}$ (S)[c]	$-nRT$ ln[S][d]	$\Delta G^\circ_{ex,S}(X)$ model 1[a]	$\Delta G^\circ_{ex,S}(X)$ model 2[b]	$T\Delta S^\circ_{ig,form}(S_n\cdot X)$ model 2[e]
				S = MeOH				
Cl^-	0	0	−310	0	0	−310	−310	0
$(MeOH)_1\cdot Cl^-$	−60	−38	−281	27	−8	−322	−301	−24
$(MeOH)_2\cdot Cl^-$	−112	−44	−258	54	−16	−332	−264	−74
$(MeOH)_3\cdot Cl^-$	−159	−44	−243	81	−24	−345	−230	−122
$(MeOH)_4\cdot Cl^-$	−200	−37	−231	108	−32	−356	−192	−173
$(MeOH)_5\cdot Cl^-$	−236	−23	−225	135	−40	−365	−153	−225
$(MeOH)_6\cdot Cl^-$	−270	−7	−219	162	−48	−375	−112	−277
				S = MeCN				
Cl^-	0	0	−311	0	0	−311	−311	0
$(MeCN)_1\cdot Cl^-$	−49	−30	−281	26	−7	−312	−292	−22
$(MeCN)_2\cdot Cl^-$	−94	−28	−256	52	−15	−314	−247	−72
$(MeCN)_3\cdot Cl^-$	−134	−22	−241	77	−22	−320	−208	−119
$(MeCN)_4\cdot Cl^-$	−171	−10	−228	103	−29	−325	−164	−171
$(MeCN)_5\cdot Cl^-$	−211	0	−215	129	−37	−334	−123	−223
$(MeCN)_6\cdot Cl^-$	−238	23	−219	155	−44	−347	−85	−276
				Δ (MeOH−MeCN)				
Cl^-	0	0	1	0	0	**1**	**1**	0
$(S)_1\cdot Cl^-$	−10	−8	−1	1	−1	**−10**	**−8**	−2
$(S)_2\cdot Cl^-$	−18	−16	−2	2	−1	**−19**	**−17**	−2
$(S)_3\cdot Cl^-$	−25	−22	−2	4	−2	**−25**	**−22**	−3
$(S)_4\cdot Cl^-$	−29	−27	−4	5	−3	**−31**	**−28**	−2
$(S)_5\cdot Cl^-$	−25	−23	−10	6	−3	**−32**	**−30**	−2
$(S)_6\cdot Cl^-$	−31	−30	0	7	−4	**−28**	**−27**	−1

[a] Model 1 includes only electronic degrees of freedom. [b] Model 2 includes electronic, rotational, and translational degrees of freedom. [c] $\Delta G^\circ_{ex,S}$ (MeOH) = −27.0 kJ/mol; $\Delta G^\circ_{ex,S}$ (MeCN) = −25.8 kJ/mol. [d] RT ln[MeOH] = 8.0 kJ/mol; RT ln[MeCN] = 7.3 kJ/mol. [e] $\Delta S^\circ_{ig,form}$ ($S_n\cdot X$) = 0 for model 1.

TABLE 4: Energetics (kJ/mol) of Methanol Molecule (X = MeOH) Solvation in Methanol and Acetonitrile with Gas Phase, and SS(V)PE Calculations Are Performed at MP2/6-31(+,+)G(d, p) and HF/6-31(+,+)G(d, p) Levels of Theory, Respectively

	$\Delta G^\circ_{ig,form}(S_3\cdot X)$ model 1[a]	$\Delta G^\circ_{ig,form}(S_3\cdot X)$ model 2[b]	$\Delta G^\circ_{ex,S}(S\cdot X)$	$-3^*\Delta G^\circ_{ex,S}$ (S)	-3^*RT ln[S]	$\Delta G^\circ_{ex,S}(X)$ model 1[a]	$\Delta G^\circ_{ex,S}$ (X) model 2[b]
$(MeOH)_3\cdot MeOH$	−75	58	−44	81	−24	−62	72
$(MeCN)_3\cdot MeOH$	−47	85	−61	77	−22	−52	79
Δ(MeOH−MeCN)	−29	−26	17	4	−2	−10	−8

[a] Model 1 includes only electronic degrees of freedom. [b] Model 2 includes electronic, rotational, and translational degrees of freedom.

of methanol and acetonitrile (Table 3). With only one solvent molecule, the chloride solvation is energetically more favorable in methanol than in acetonitrile by approximately 10 kJ/mol. Inclusion of more solvent molecules makes this effect more pronounced and the absolute value of $\Delta\Delta G^\circ_{ex}(Cl^-)$ increases with the number of solvent molecules. The final value of $\Delta\Delta G^\circ_{ex}(Cl^-)$ obtained for clusters with 4, 5, and 6 solvent molecules is around −30 kJ/mol.

Examination of the energy components of the $\Delta\Delta G^\circ_{ex}(Cl^-)$ shows that $\Delta\Delta G^\circ_{ig,form}(S_n\cdot Cl^-)$ is the major contributor to the final solvation energies. Therefore, the better solvation of the chloride anion in methanol is a consequence of stronger specific bonds formed with the first shell of solvent molecules. The binding energy per solvent molecule in methanol clusters with n = 4, 5, and 6 is around 6 kJ/mol larger than in corresponding acetonitrile clusters. The rest of the components of $\Delta\Delta G^\circ_{ex}(Cl^-)$, responsible for long-range interaction effects, tend to cancel each other and contribute only slightly to the final values of $\Delta\Delta G^\circ_{ex}(Cl^-)$.

3.3. $\Delta\Delta G^\circ_{ex}$(MeOH). The absolute solvation energies of methanol (methanol participates in reaction R1 as a reactant) are calculated for both solvents using eq 6. The results are summarized in Table 4, and the shapes of the clusters are shown in Figure 2. The final value of $\Delta\Delta G^\circ_{ex}$(MeOH) is a result of two opposing effects. On one side, methanol−methanol hydrogen bonds are stronger than methanol−acetonitrile hydrogen bonds ($\Delta\Delta G^\circ_{ig,form}(S_3\cdot MeOH) < 0$) because OH groups in methanol−methanol interactions are more polar than CH groups in methanol−acetonitrile interactions. On the other side, the methanol−acetonitrile cluster is more strongly stabilized by the polarizable continuum ($\Delta\Delta G^\circ_{ex,S}(S_3\cdot MeOH) > 0$) because two polar CN groups are exposed to the solute−continuum interaction. As a result, the calculated solvation free energy of a methanol molecule is approximately 10 kJ/mol lower in methanol than in acetonitrile.

3.4. Summary: $\Delta\Delta G^\circ$. The difference in ΔG°_S for reaction R1 occurring in methanol and acetonitrile can be calculated as a sum of four terms in eq 5 discussed above. In summarizing the results of the previous sections, we can estimate these energy terms as follows:

$$\Delta\Delta G^\circ_{ex}(MeOH) \approx -10 \text{ kJ/mol}$$

$$\Delta\Delta G^\circ_{ex}(PFeCl) \approx -6 \text{ kJ/mol}$$

$$\Delta\Delta G^\circ_{ex}(PFe(HOMe)^+) \approx -9 \text{ kJ/mol}$$

$$\Delta\Delta G^\circ_{ex}(Cl^-) \approx -30 \text{ kJ/mol}$$

Thus, the final estimate for the difference in the dissociation free energies in methanol and acetonitrile is $\Delta\Delta G^\circ \approx -23$ kJ/

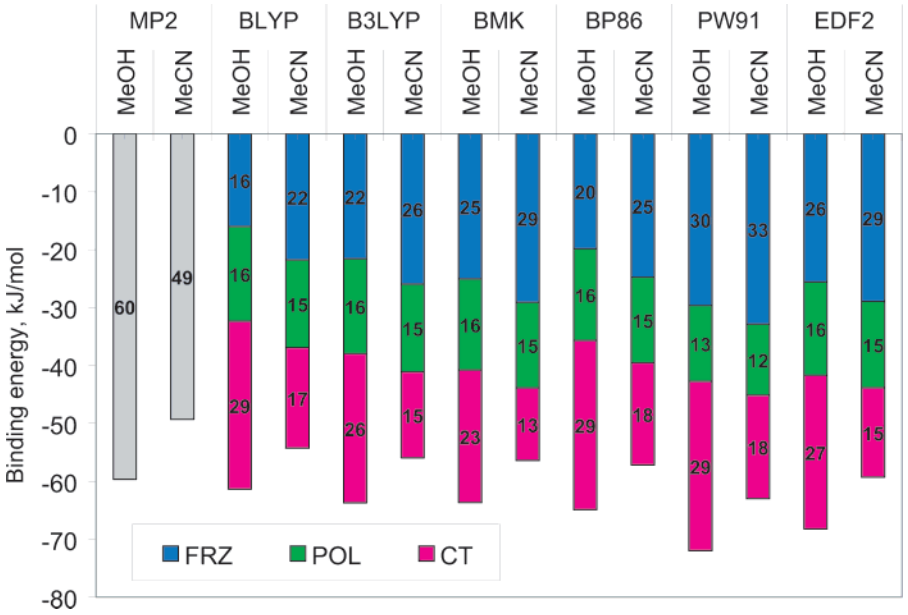

Figure 4. Energy decomposition analysis of chloride−solvent interactions in $S_1 \cdot Cl^-$; S is MeOH and MeCN. Basis set is 6-31(+,+)G(d, p). Geometries are optimized at the MP2/6-31(+,+)G(d, p) level.

mol, in a very good agreement with the experimental value of −21 kJ/mol.

Therefore, despite the simplicity of the quasichemical model, the origin of the strong solvent effect on the dissociation of PFeCl can be understood. The dissociation is energetically more favorable in methanol than in acetonitrile primarily because of the strong specific interactions between the chloride anion and the solvent methanol molecules in its first solvation shell. These interactions are weaker in acetonitrile. The differences in the solvation energies of the other species participating in the dissociation process are also noticeable but contribute to the observed solvent effect to a lesser extent.

3.5. Energy Decomposition Analysis of Chloride−Solvent Interactions. The nature of chloride−solvent interactions is studied in detail with a recently proposed energy decomposition method.[32] Decomposition of the total solvent−chloride binding energies in $S_1 \cdot Cl^-$ is shown in Figure 4 together with the MP2 binding energies which cannot be readily decomposed. Although none of the density functionals tested in this work reproduces the MP2 energy exactly, the DFT energies reported in Figure 4 are in reasonable agreement with the MP2 results. Most importantly for our present purpose, the difference between the MP2 binding energies for methanol and acetonitrile (−10 kJ/mol) is captured well by DFT.

From Figure 4, we see that the different density functionals all produce rather different absolute values for the different components of the interaction energy and indeed for the total interaction energy. This partly reflects differences between the functionals and also reflects the fact that charge-transfer and frozen density interactions depend exponentially on interfragment distances. Fortunately, however, the differences in both the total interaction energies and the components of the interaction energy are quite stable to the choice of density functional and therefore can be discussed with confidence. $\Delta\Delta E_{FRZ} \approx 3-6$ kJ/mol indicating that frozen density interactions are stronger in acetonitrile, most likely because of the higher dipole moment of the acetonitrile molecule ($\mu_{MeOH} =$ 1.70 D, $\mu_{MeCN} = 3.92$ D). The polarization energy component is the same in both solvents ($\Delta\Delta E_{POL} \approx -1$ kJ/mol); however, charge-transfer effects contribute approximately 10−12 kJ/mol more into the chloride−methanol binding energy than into the chloride−acetonitrile binding energy. Therefore, it is the large contribution of charge-transfer effects that leads to stronger chloride−methanol binding compared with chloride−acetonitrile binding. It is worth noting that the charge is primarily transferred from the chloride anion to the solvent molecule ($\Delta E_{CT}^{Cl^- \rightarrow S}$:$\Delta E_{CT}^{S \rightarrow Cl^-} = 98$:2).

3.6. Comment on the Absolute Solvation Energies and Entropy Effects. In this work, we used a simple form of the quasichemical approximation[17,20] to evaluate the absolute free energies of solvation of several molecular and ionic species in methanol and in acetonitrile. Even though the calculation of the absolute free energies of solvation was not the main goal of this work, we would like to make some comments on the performance of the quasichemical method for these systems.

The absolute solvation free energies of the chloride anion in methanol and acetonitrile ($\Delta G^\circ_{ex,S}(Cl^-)$) are shown in Table 3. Models with different numbers of explicit solvent molecules ($n = 0-6$) were used. It is clear that the free energy values of $\Delta G^\circ_{ex,S}(Cl^-)$ calculated with the thermal correction for rotational and translational degrees of freedom (model 2) increase rapidly with n. Therefore, it is hard to assign any particular value to $\Delta G^\circ_{ex,S}(Cl^-)$ if model 2 is used. The reason for such a strong dependence on n in model 2 is that the ideal gas free energy of cluster formation, $\Delta G^\circ_{ig,form}(S_n \cdot Cl^-)$ is calculated within the rigid-molecule approximation (see above). If this approximation is used with model 2, rotational and translational motion of free solvent molecules become completely "frozen" upon formation of the cluster. This leads to a significant overestimation of the entropy effects of cluster formation. Calculated $\Delta G^\circ_{ig,form}(S_n \cdot Cl^-)$ values are large negative numbers (Table 3). Therefore, the stability of the cluster is underestimated in this approach mainly because of the entropic component. Moreover, the error in the calculated thermodynamic functions grows with n, and thus, the results become less reliable for solutes with large number of solvent molecules in the first solvation shell.

By completely neglecting rotations and translations, we introduce the opposite extreme approximation (model 1), ensemble of fixed rigid noninteracting molecules, for which $\Delta S^\circ_{ig,form}(S_n \cdot Cl^-)$ is equal to zero. As shown in Table 3,

solvation free energies predicted by model 1 decrease only slightly with n (as opposed to the rapid increase observed for model 2). Unlike model 2, which "freezes out" the internal low-frequency modes in the cluster but allow the corresponding rotations and translations in the separated solute/solvent, model 1 prohibits them for both the cluster and the separated solute/solvent. This equal treatment of translations and rotations is the main reason for a seemingly better performance of model 1.

The true values of $\Delta S^{\circ}_{ig,form}(S_n \cdot Cl^-)$ are expected to lie in between two limits given by models 1 and 2. These true values will produce $\Delta G^{\circ}_{ex,S}(Cl^-)$ that will not depend on n and will fall in between the $\Delta G^{\circ}_{ex,S}(Cl^-)$ values for models 1 and 2. However, the estimation of the true value of $\Delta S^{\circ}_{ig,form}(S_n \cdot Cl^-)$ is a complicated computational problem that is beyond the scope of this work.

Therefore, we can conclude that, in order to compute absolute solvation energies with quasichemical methods, special care must be taken when computing the ideal gas entropy of cluster formation. In the case of PFeCl dissociation, the experimental measurements show that entropy effects (ΔS°) are the same for methanol and acetonitrile. Even though neither model 1 nor model 2 can precisely capture absolute values of solvation entropy, the errors cancel out when the difference between two solvents, $\Delta\Delta S^{\circ}$, is calculated. Therefore, one might expect a good agreement between the calculated and the experimentally measured values for $\Delta\Delta G^{\circ}$.

4. Conclusions

Experimental measurements have shown that the free energy of dissociation of PFeCl is 21 kJ/mol lower in methanol than in acetonitrile. In order to understand the origin of the strong solvent effect on the thermodynamics of this process, we studied the energetics of the dissociation of PFeCl computationally using mixed discrete/continuum models. In these models, solute and a few solvent molecules in the first solvation shell are treated with accurate ab initio methods, and the remaining solvent is described by the dielectric continuum.

The calculated difference in the dissociation free energies is approximately 23 kJ/mol lower in methanol than in acetonitrile, in full agreement with the experimental measurements. The origin of the solvent effect on the dissociation reaction is primarily due to the difference in the energy of solvation of the chloride anion. The hydrogen bonds formed by methanol molecules with Cl^- are stronger than acetonitrile−chloride interactions. Energy decomposition analysis of chloride−solvent interactions suggests that this is because of a higher contribution of charge delocalization effects to the chloride−methanol bonding.

Although the simple quasichemical approximation used in this work does not reproduce the entropy effects of solvation, the final calculated values of $\Delta\Delta G^{\circ}$ reproduce experimental results very well because the entropy of solvation is the same for both solvents (i.e., $\Delta\Delta S^{\circ}$ is close to zero).

Acknowledgment. This work was supported by the Director, Office of Basic Energy Sciences, Chemical Sciences Division of the U.S. Department of Energy under Contract No. DE-AC03-76SF00098 and by the National Science Foundation under Grant CHE-0535710.

References and Notes

(1) Stephenson, N. A.; Bell, A. T. *J. Am. Chem. Soc.* **2005**, *127* (24), 8635−8643.

(2) Stephenson, N. A.; Bell, A. T. *Inorg. Chem.* **2006**, *45* (14), 5591−5599.

(3) Frenkel, D.; Smit, B. *Understanding Molecular Simulation: From Algorithms to Applications;* Academic Press: Orlando, FL, 2001.

(4) Kollman, P. *Chem. Rev.* **1993**, *93* (7), 2395−2417.

(5) Kofke, D. A.; Cummings, P. T. *Mol. Phys.* **1997**, *92* (6), 973−996.

(6) Vangunsteren, W. F.; Berendsen, H. J. C. *Angew. Chem., Int. Ed. Engl.* **1990**, *29* (9), 992−1023.

(7) Tuckerman, M. E.; Martyna, G. J. *J. Phys. Chem. B* **2000**, *104* (2), 159−178.

(8) Sun, H. *J. Phys. Chem. B* **1998**, *102* (38), 7338−7364.

(9) Grossfield, A.; Ren, P. Y.; Ponder, J. W. *J. Am. Chem. Soc.* **2003**, *125* (50), 15671−15682.

(10) Wood, R. H. *J. Chem. Phys.* **1995**, *103* (14), 6177−6187.

(11) Hummer, G.; Pratt, L. R.; Garcia, A. E. *J. Phys. Chem. A* **1998**, *102* (41), 7885−7895.

(12) Tomasi, J.; Persico, M. *Chem. Rev.* **1994**, *94* (7), 2027−2094.

(13) Cramer, C. J.; Truhlar, D. G. *Chem. Rev.* **1999**, *99* (8), 2161−2200.

(14) Tomasi, J.; Mennucci, B.; Cammi, R. *Chem. Rev.* **2005**, *105* (8), 2999−3093.

(15) *CRC Handbook of Chemistry and Physics;* CRC Press: Boca Raton, FL, 2005.

(16) Pliego, J. R.; Riveros, J. M. *J. Phys. Chem. A* **2001**, *105* (30), 7241−7247.

(17) Westphal, E.; Pliego, J. R. *J. Chem. Phys.* **2005**, *123* (7), 074508.

(18) Grabowski, P.; Riccardi, D.; Gomez, M. A.; Asthagiri, D.; Pratt, L. R. *J. Phys. Chem. A* **2002**, *106* (40), 9145−9148.

(19) Asthagiri, D.; Pratt, L. R.; Kress, J. D.; Gomez, M. A. *Chem. Phys. Lett.* **2003**, *380* (5−6), 530−535.

(20) Asthagiri, D.; Pratt, L. R.; Ashbaugh, H. S. *J. Chem. Phys.* **2003**, *119* (5), 2702−2708.

(21) Asthagiri, D.; Pratt, L. R.; Paulaitis, M. E.; Rempe, S. B. *J. Am. Chem. Soc.* **2004**, *126* (4), 1285−1289.

(22) Rempe, S. B.; Asthagiri, D.; Pratt, L. R. *Phys. Chem. Chem. Phys.* **2004**, *6* (8), 1966−1969.

(23) Paulaitis, M. E.; Pratt, L. R. *Adv. Protein Chem.* **2002**, *62*, 283−310.

(24) Shao, Y.; Molnar, L. F.; Jung, Y.; Kussmann, J.; Ochsenfeld, C.; Brown, S. T.; Gilbert, A. T. B.; Slipchenko, L. V.; Levchenko, S. V.; O'Neill, D. P.; DiStasio, R. A.; Lochan, R. C.; Wang, T.; Beran, G. J. O.; Besley, N. A.; Herbert, J. M.; Lin, C. Y.; Van Voorhis, T.; Chien, S. H.; Sodt, A.; Steele, R. P.; Rassolov, V. A.; Maslen, P. E.; Korambath, P. P.; Adamson, R. D.; Austin, B.; Baker, J.; Byrd, E. F. C.; Dachsel, H.; Doerksen, R. J.; Dreuw, A.; Dunietz, B. D.; Dutoi, A. D.; Furlani, T. R.; Gwaltney, S. R.; Heyden, A.; Hirata, S.; Hsu, C. P.; Kedziora, G.; Khalliulin, R. Z.; Klunzinger, P.; Lee, A. M.; Lee, M. S.; Liang, W.; Lotan, I.; Nair, N.; Peters, B.; Proynov, E. I.; Pieniazek, P. A.; Rhee, Y. M.; Ritchie, J.; Rosta, E.; Sherrill, C. D.; Simmonett, A. C.; Subotnik, J. E.; Woodcock, H. L.; Zhang, W.; Bell, A. T.; Chakraborty, A. K.; Chipman, D. M.; Keil, F. J.; Warshel, A.; Hehre, W. J.; Schaefer, H. F.; Kong, J.; Krylov, A. I.; Gill, P. M. W.; Head-Gordon, M. *Phys. Chem. Chem. Phys.* **2006**, *8* (27), 3172−3191.

(25) Adamson, R. D.; Gill, P. M. W.; Pople, J. A. *Chem. Phys. Lett.* **1998**, *284* (1−2), 6−11.

(26) Moller, C.; Plesset, M. S. *Phys. Rev.* **1934**, *46* (7), 618−622.

(27) Head-Gordon, M. *Mol. Phys.* **1999**, *96* (4), 673−679.

(28) Boys, S. F.; Bernardi, F. *Mol. Phys.* **1970**, *19* (4), 553−566.

(29) Hill, T. L. *An introduction to statistical thermodynamics;* Dover Publications: New York, 1986.

(30) Ben-Naim, A. *J. Phys. Chem.* **1978**, *82* (7), 792−803.

(31) Chipman, D. N. *Theor. Chem. Acc.* **2002**, *107* (2), 80−89.

(32) Khaliullin, R. Z.; Cobar, E. A.; Lochan, R. C.; Bell, A. T.; Head-Gordon, M. *J. Phys. Chem. B* **2007**, in press.

(33) Becke, A. D. *J. Chem. Phys.* **1993**, *98* (7), 5648−5652.

(34) Lee, C. T.; Yang, W. T.; Parr, R. G. *Phys. Rev. B* **1988**, *37* (2), 785−789.

(35) Becke, A. D. *Phys. Rev. A* **1988**, *38* (6), 3098−3100.

(36) Perdew, J. P. *Phys. Rev. B* **1986**, *33* (12), 8822−8824.

(37) Boese, A. D.; Martin, J. M. L. *J. Chem. Phys.* **2004**, *121* (8), 3405−3416.

(38) Perdew, J. P.; Burke, K.; Wang, Y. *Phys. Rev. B* **1996**, *54* (23), 16533−16539.

(39) Lin, C. Y.; George, M. W.; Gill, P. M. W. *Aust. J. Chem.* **2004**, *57* (4), 365−370.